Report

SOURCE DATA | TRANSPARENT PROCESS

EMBO reports

The novel lncRNA *CALIC* upregulates AXL to promote colon cancer metastasis

Yoshihiro Kawasaki[1,*], Masaya Miyamoto[1], Takeaki Oda[1], Kosuke Matsumura[1], Lumi Negishi[1], Ryuichiro Nakato[2], Sakiko Suda[1], Naoko Yokota[2], Katsuhiko Shirahige[2] & Tetsu Akiyama[1]

Abstract

Long non-coding RNAs (lncRNAs) are aberrantly expressed in many disease conditions, including cancer. Accumulating evidence indicates that some lncRNAs may play critical roles in cancer progression and metastasis. Here, we identify a set of lncRNAs that are upregulated in metastatic subpopulations isolated from colon cancer HCT116 cells *in vivo* and show that one of these lncRNAs, which we name *CALIC*, is required for the metastatic activity of colon cancer cells. We show that *CALIC* associates with the RNA-binding protein hnRNP-L and imparts specificity to hnRNP-L-mediated gene expression. Furthermore, we demonstrate that the *CALIC*/hnRNP-L complex upregulates the tyrosine kinase receptor AXL and that knockdown of *CALIC* or AXL using shRNA in colon cancer cells attenuates their ability to form metastases in mice. These results suggest that the *CALIC*/hnRNP-L complex enhances the metastatic potential of colon cancer cells.

Keywords cancer metastasis; lncRNA; signal transduction
Subject Categories Cancer; RNA Biology
DOI 10.15252/embr.201847052 | Received 14 September 2018 | Revised 29 May 2019 | Accepted 18 June 2019 | Published online 29 July 2019
EMBO Reports (2019) 20: e47052

Introduction

Recent advances in genomic research have revealed that only 1.2% of the mammalian genome encodes proteins, while the remaining portion is transcribed to generate an enormous number of non-coding RNAs (ncRNAs) [1–3]. These ncRNAs are currently divided into two main classes based on their transcript size: small ncRNAs (20–200 nucleotides) and long ncRNAs (lncRNAs, > 200 nucleotides) [4]. These newly discovered lncRNAs have emerged as a major class of regulatory molecules associated with a broad range of biological processes and diseases [5–12]. LncRNAs have been proposed to regulate gene expression by various mechanisms, including acting as scaffolds for chromatin modifiers, transcriptional regulators, microRNA sponges, protein decoys, and enhancers. Often, these functions of lncRNAs are mediated through complex formation with protein partners.

It is estimated that 90% of the deaths caused by solid tumors are due to metastases, which display marked variability in their clinical manifestations. For example, liver and lung metastases are major contributors to the mortality of colon cancer patients. This process of tumor metastasis consists of a series of steps that relocate tumor cells from the primary neoplasm to a distant location. Typically, tumor cells invade the local tissue surrounding the primary tumor (invasion), enter the microvasculature of the lymph and blood systems (intravasation), and then survive in the circulation. These tumor cells can then exit from circulation and invade into the microenvironment of distant tissues (extravasation), where they now begin to grow (colonization) [13,14]. Metastasis to distant sites is usually dependent on the tumor cells' intrinsic abilities to proliferate, survive, and migrate.

The receptor tyrosine kinase AXL plays critical roles in tumor cell migration and invasion through the regulation of FAK1, Rho family GTPases, and the GTP exchange factor Vav1 [15,16]. AXL also plays roles in regulating cell growth, survival, and drug resistance via the ERK and PI3K pathways in both normal and cancer cells [17,18]. AXL is overexpressed in a wide variety of cancers, and it is thus considered as a potential therapeutic target. In this study, we identify a novel lncRNA that is significantly upregulated in subpopulations of HCT116 cells that were selected for elevated metastatic activity. We have designated this lncRNA *CALIC* (cancer metastasis-associated long intergenic non-coding RNA) and show that it associates with the RNA-binding protein hnRNP-L (heterogeneous nuclear ribonucleoprotein-L) and upregulates AXL, thereby promoting migration and metastasis of colon cancer cells.

Results and Discussion

CALIC is upregulated in metastatic subpopulations

In vivo selection schemes have proven effective for the isolation of highly metastatic subpopulations from heterogeneous cancer cell lines and the identification of genes linked to the metastatic behavior [19,20]. HCT116 colon cancer cells were injected intravenously

1 Laboratory of Molecular and Genetic Information, Institute for Quantitative Biosciences, The University of Tokyo, Bunkyo-ku, Tokyo, Japan
2 Laboratory of Genome Structure and Function, Institute for Quantitative Biosciences, The University of Tokyo, Bunkyo-ku, Tokyo, Japan
*Corresponding author. Tel: +81 3 5841 7835; Fax: +81 3 5841 8482; E-mail: kawasaki@iam.u-tokyo.ac.jp

into the tail veins of immunodeficient mice, and pulmonary metastases were isolated. To identify lncRNAs involved in metastatic progression, we compared gene expression patterns between the parental cells and the metastatic subpopulations selected *in vivo* (Fig 1A). RNA-Seq and gene ontology (GO) analyses revealed that 2,819 genes were upregulated (FDR < 0.05, logFC > 1, TPM > 5) in metastatic subpopulations (Dataset EV1) and highly associated with cell motility (Figs 1B, and EV1A and B). These included 300 non-coding genes annotated by Ensemble, among which 129 were designated as long intergenic non-coding RNAs (lincRNAs) in the GENCODE v27 annotation dataset. From these, we selected 11 lincRNAs that were expressed at high levels and were easy to handle (FDR < 0.05, logFC > 1.3, TPM > 25, < 3,000 bp in length).

We first examined whether siRNA-mediated knockdown of any of the 11 lincRNAs affects the motility of HCT116 cells using Transwell migration chambers. We found that knockdown of *LINC00920* caused the most significant decrease in cell migration, and we named this lincRNA *CALIC* (Figs 1C and D, and EV1C). In addition, RNA-Seq and Gene Ontology (GO) analyses of HCT116 cells in which *CALIC* had been knocked down using siRNA revealed that *CALIC* target genes were enriched for those involved in "cell motility" and "localization of cell" (Fig 1E). Consistent with the results

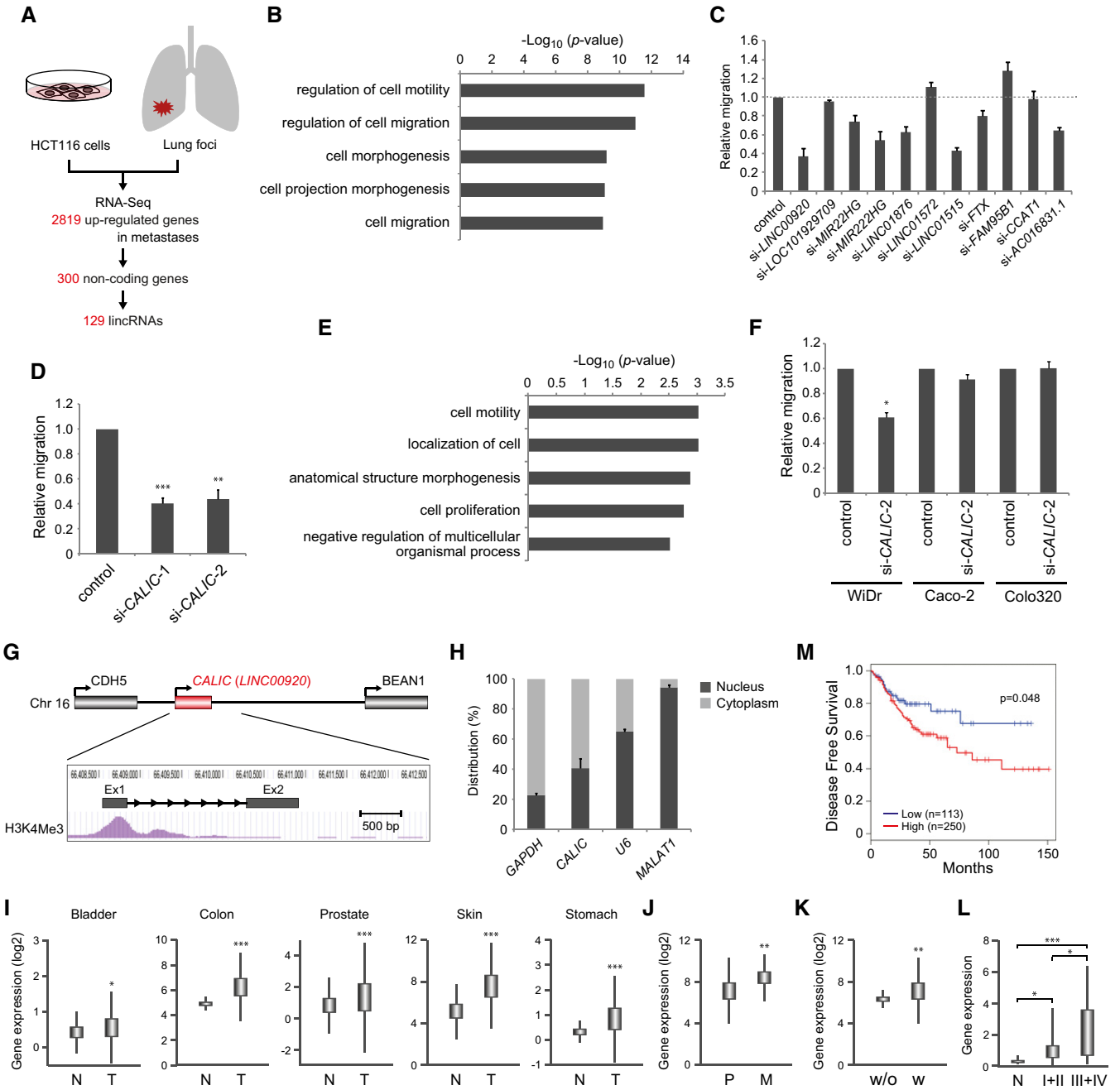

Figure 1.

Figure 1. Identification of *CALIC* as a lincRNA upregulated in selected subpopulations having elevated metastatic activity.

A Schematic representation of the experimental method used to identify lincRNAs upregulated in metastatic subpopulations isolated from HCT116 colon cancer cells.
B Gene ontology (GO) analysis of upregulated genes in metastatic lesions.
C Cell migration assays were performed using Transwell migration chambers. HCT116 cells were transfected with siRNAs targeting 11 candidate lincRNAs, and cell migration activities were evaluated by Transwell migration assays (n = 3). *CALIC* is the lincRNA targeted by si-*LINC00920*.
D Migration of HCT116 cells transfected with the indicated siRNAs or negative control (n = 4).
E GO analysis of differentially expressed genes in *CALIC* knockdown HCT116 cells.
F Migration of colon cancer cells treated with an siRNA targeting *CALIC* (n = 3).
G (Top) Schematic representation of the chromosomal location of the *CALIC* gene locus. Arrows indicate the orientation of transcription. (Bottom) ENCODE ChIP-seq data for H3K4Me3 is displayed in the UCSC browser illustrations. Gray boxes mark locations of exons (Ex1–2) of *CALIC*.
H Subcellular localization analysis of *CALIC*. RNAs were isolated from the nuclear and cytoplasmic fractions of HCT116 cells and quantified by qRT–PCR (n = 3). Nuclear controls: *U6*, *MALAT1*; cytoplasmic control: *GAPDH*.
I *CALIC* expression levels in cancer tissues. N, normal mucosa; T, tumor. Bladder (n = 387), Colon (n = 40), Prostate (n = 542), Skin (n = 62), Stomach (n = 383).
J Expression of *CALIC* in primary skin tumors (P) and their metastases (M) (n = 56).
K Expression of *CALIC* in primary skin tumors of patients without (w/o) or with (w) metastases (n = 42).
L qRT–PCR analysis of *CALIC* expression in early (I/II) and late (III/IV) stage colon cancers [normal (N) n = 8, stage I/II n = 14, stage III/IV n = 26].
M Kaplan–Meier curves for disease-free survival of colon cancer patients whose primary tumors expressed low (blue, n = 113) or high (red, n = 250) levels of *CALIC*. Statistical analysis was performed using the log-rank test.

Data information: Results are expressed as the mean ± SEM. *$P < 0.05$, **$P < 0.01$, ***$P < 0.001$ (Student's t-test).

obtained with HCT116 cells, *CALIC* knockdown inhibited the migration of highly metastatic WiDr colon cancer cells expressing *CALIC* at high levels (Figs 1F and EV1D and E). In contrast, *CALIC* knockdown barely affected the migration of poorly metastatic Caco-2 and Colo320 colon cancer cells expressing low levels of *CALIC* (Fig 1F).

The *CALIC* gene is 913 bp in length, containing two exons, and is located between the CDH5 (cadherin-5) and BEAN1 (brain-expressed protein associating with Nedd4 homolog) genes (Fig 1G) on human chromosome 16. Analysis of ENCODE (Encyclopedia of DNA Elements) ChIP-seq data from epidermal keratinocytes (NHEK) revealed that H3K4 trimethylation (H3K4me3), a mark associated with active transcription, is enriched at the transcription start site of *CALIC* (Fig 1G). The full-length transcript has no protein-coding potential according to the Coding Potential Calculator (CPC) [21] and Coding Potential Assessment Tool (CPAT) [22]. We also investigated the subcellular localization of *CALIC* in HCT116 cells by measuring the ratio of its abundance in the nucleus versus the cytoplasm using quantitative reverse transcription–PCR (qRT–PCR). We observed that *CALIC* was localized in both the cytoplasm and nucleus, while the lncRNA *MALAT1* localized mainly in the nucleus as reported previously [23] (Figs 1H and EV1F).

To determine whether *CALIC* expression is altered in human cancers, gene expression data from patients were analyzed by the HCMDB (Human Cancer Metastasis Database) Web server program (http://hcmdb.i-sanger.com/index) [24]. We observed that *CALIC* was upregulated in many cancers, including bladder, colon, prostate, skin, and gastric cancers (Fig 1I). Of note, *CALIC* expression in skin cancer was significantly higher in metastases than in primary tumors (Fig 1J). Furthermore, *CALIC* expression was clearly elevated in primary tumors of patients who had developed metastases compared to those without metastases (Fig 1K). In addition, qRT–PCR analysis of a colon cancer cDNA panel (OriGene) showed that *CALIC* expression was higher in late stage than in early stage cancers, while no statistically significant difference was detected between *CALIC* expression and other factors such as age, gender, or histological differentiation (Figs 1L and EV1G–I). Moreover, high *CALIC* expression in colon cancer was associated with an increased risk for tumor relapse, although overall survival did not differ significantly (Figs 1M and EV1J). These results raise the possibility that *CALIC* is involved in the motility and metastasis of cancer cells.

CALIC interacts with hnRNP-L

To investigate the molecular mechanisms by which *CALIC* plays a role in metastasis, we attempted to identify proteins that may interact with *CALIC* by an RNA pull-down method. Proteins that co-precipitated with *in vitro* synthesized *CALIC*, but not with antisense *CALIC*, were separated by SDS–PAGE and analyzed by mass spectrometry (Fig 2A). Among five protein candidates identified, the protein with the highest SEQUEST score was hnRNP-L, a multifunctional RNA-binding protein involved in various biological processes such as transcription, splicing, and translation [25–32] (Table EV1). Immunoblotting analysis confirmed that hnRNP-L specifically co-precipitated with the sense strand of *CALIC* (Fig 2B). Deletion analysis revealed that hnRNA-L interacted with a 5′ fragment of *CALIC* (nucleotides 1–295), which contains two ACACA motifs, potential consensus binding sites for hnRNP-L [32] (Fig 2B). We therefore generated a *CALIC* mutant (*CALIC*-mut) in which the two ACACA motifs were replaced with TTTTT, and found that *CALIC*-mut barely interacted with hnRNP-L (Fig 2B). Thus, hnRNP-L may associate with *CALIC* via these ACACA motifs. We also performed RNA immunoprecipitation (RIP) assays with anti-hnRNP-L antibody using lysates from HCT116 or LS180 colon cancer cells. qRT–PCR analysis of the immunoprecipitates revealed that hnRNP-L was associated with endogenous *CALIC*, but not with *HPRT1* and *MALAT1* (Fig 2C and D). In a parallel experiment, we confirmed that hnRNP-L was also associated with the lncRNA *THRIL* as reported previously [28]. Furthermore, immunoblotting of chromatin isolation by RNA purification (ChIRP) products generated using *CALIC* antisense oligos detected hnRNP-L associated with *CALIC in vivo* (Figs 2E and EV1K). In addition, knockdown of hnRNP-L using siRNA resulted in the decreased motility of HCT116 cells (Figs 2F and EV1L). These results suggest that *CALIC* is associated with hnRNP-L, which is involved in the motility of colon cancer cells.

CALIC imparts specificity to hnRNP-L-mediated gene expression

To clarify the effect of *CALIC* on the function of hnRNP-L, we performed RNA-Seq experiments using HCT116 cells transfected with two different siRNAs targeting hnRNP-L or *CALIC*. We selected only the transcripts that were affected by both of the

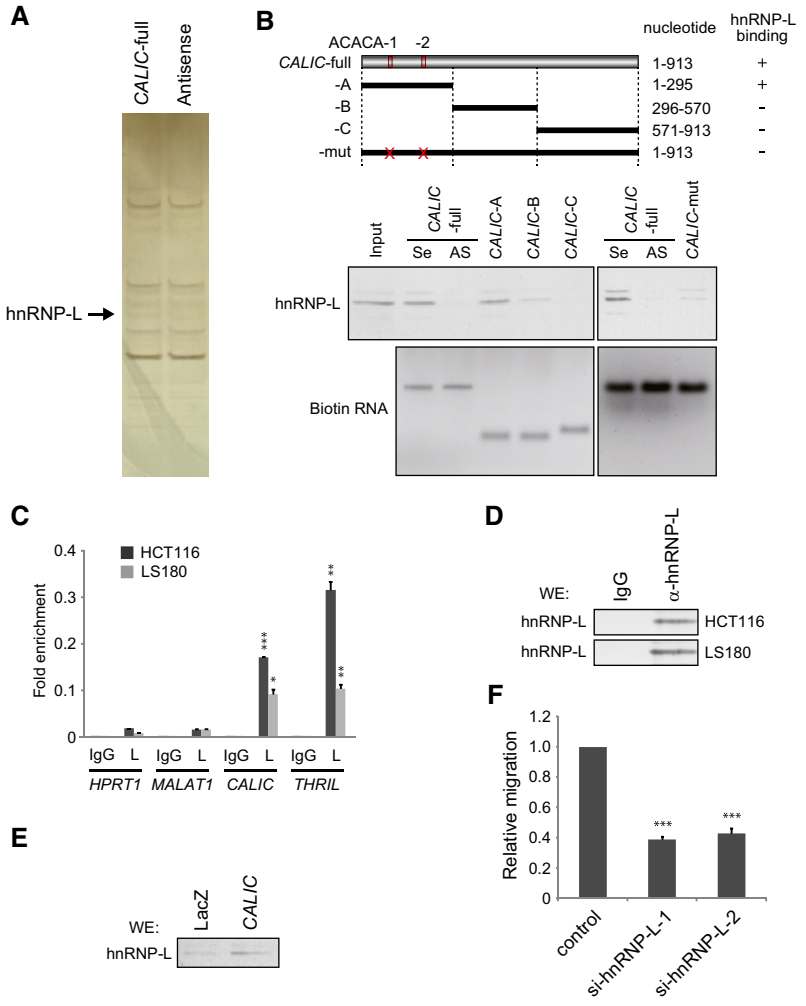

Figure 2. *CALIC* interacts with hnRNP-L.

A Biotinylated full-length *CALIC* or antisense *CALIC* (negative control) generated *in vitro* was incubated with lysates from DLD-1 colon cancer cells and precipitated with streptavidin beads. Precipitated proteins were resolved by SDS–PAGE followed by silver staining. The protein band indicated by the arrow was excised and subjected to mass spectrometry.

B (Top) schematic of the full-length and mutants of *CALIC* used for the precipitation of hnRNP-L from HCT116 cell lysates. The mutated elements are indicated by the cross marks. Se, sense transcript; AS, antisense transcript. +, detectable binding activity; −, no detectable activity. (Bottom) precipitated hnRNP-L and biotin-labeled fragments of *CALIC* are shown.

C, D RIP analysis was performed using control rabbit IgG or anti-hnRNP-L antibody. *HPRT1* and the lncRNA *MALAT1* were used as negative controls. Immunoblotting analysis of proteins precipitated by RIP assays using anti-hnRNP-L antibody is shown in (D) (n = 3).

E ChIRP-immunoblotting analysis of hnRNP-L association with endogenous *CALIC* in HCT116 cells.

F Migration of HCT116 cells transfected with the indicated siRNAs or negative control (n = 4).

Data information: Results are expressed as the mean ± SEM. *P < 0.05, **P < 0.01, ***P < 0.001 (Student's t-test).
Source data are available online for this figure.

two siRNAs targeting each gene in two biological replicates (P-value < 0.01, TPM > 1). We found that transcription decreased in 44% of hnRNP-L- or 54% of *CALIC*-regulated genes (Fig 3A and Dataset EV2). We also observed that 59 genes were regulated in common in both *CALIC* and hnRNP-L knockdown cells (Fig 3B). Scatter plot analysis revealed a positive correlation between the expression of these 59 genes in *CALIC* and hnRNP-L knockdown cells (Fig 3C), of which 51 (86%) were regulated in the same direction. By contrast, no significant correlation was found between the differentially expressed genes. Notably, 39 (76.5%) out of these 51 genes are common positive targets of hnRNP-L and *CALIC* (Fig 3D). GSEA analysis also revealed that genes repressed by *CALIC* knockdown were significantly overrepresented among those repressed by hnRNP-L knockdown (Fig 3E). In addition, analysis of colon and rectal cancer samples from The Cancer Genome Atlas (TCGA) dataset revealed a similar pattern of expression among genes induced in common by both *CALIC* and hnRNP-L (Fig 3F). These results suggest that *CALIC* provides specificity to hnRNP-L-induced gene expression.

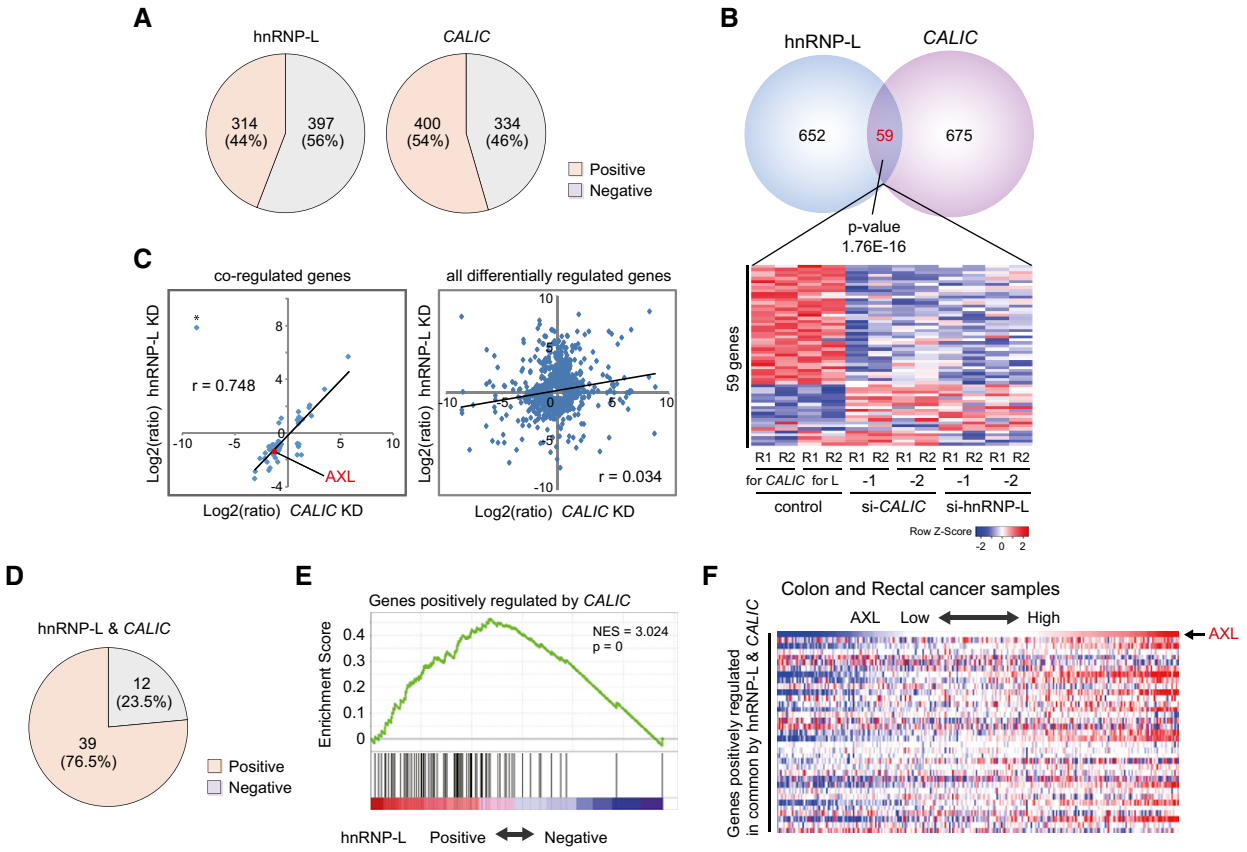

Figure 3. *CALIC* imparts specificity to hnRNP-L-mediated gene expression.

A, B RNA-Seq analysis of hnRNP-L- and *CALIC*-regulated genes in HCT116 cells. Pie chart showing genes regulated by hnRNP-L or *CALIC* (A). Venn diagram showing the overlap of genes differentially expressed by hnRNP-L (blue) or *CALIC* (purple) knockdown (B, top). Expression levels of 59 genes regulated in common in both hnRNP-L and *CALIC* knockdown cells relative to control siRNA experiments (B, bottom). Two biological replicates (R1 and R2) were included for each siRNA treatment. The number of genes within each category is indicated.

C Scatterplots showing correlations between *CALIC*- and hnRNP-L-regulated genes in (B). Left, co-regulated 59 genes; right, all differentially regulated genes. The correlation was calculated using the data except for the gene indicated by the asterisk.

D Genes regulated in common and in the same direction by hnRNP-L and *CALIC*.

E Genes induced by *CALIC* are significantly enriched in those upregulated by hnRNP-L. GSEA comparing the genes repressed by *CALIC* and hnRNP-L knockdown. NES, normalized enrichment score.

F Heatmap showing the expression levels of genes positively regulated in common by both *CALIC* and hnRNP-L in colon and rectal cancers. Samples are ordered based on the expression levels of AXL.

CALIC and hnRNP-L cooperate to induce AXL expression

We next examined the molecular mechanisms underlying *CALIC*/hnRNP-L-mediated migration of colon cancer cells. Among the genes induced in common by both, we focused on the *AXL* gene as it encodes a receptor tyrosine kinase known to play critical roles in migration, invasion, and metastasis [17,18]. qRT–PCR and immunoblotting analyses confirmed that the expression of AXL was reduced in *CALIC* or hnRNP-L knockdown HCT116 and LS180 cells (Fig 4A–D). In addition, *CALIC* knockdown did not affect the expression of hnRNP-L (Fig 4B). The effect of *CALIC* knockdown on AXL expression in LS180 cells was more significant than that observed in HCT116 cells (Fig 4B). To assess the cooperation between *CALIC* and hnRNP-L in AXL expression, we generated lentiviruses expressing wild-type *CALIC* (*CALIC*-full), *CALIC*-mut, or a deletion mutant *CALIC* (*CALIC*-296-913) lacking the hnRNP-L-binding region. We found that AXL expression was significantly enhanced in HCT116 cells infected with a lentivirus carrying *CALIC*-full compared to control cells (Figs 4E and EV2A). In contrast, AXL expression was not enhanced in HCT116 cells infected with a lentivirus carrying *CALIC*-mut or *CALIC*-296-913 (Fig 4E). These results suggest that *CALIC* and hnRNP-L cooperate to induce AXL expression in HCT116 cells. On the other hand, AXL expression was not increased by *CALIC*-full in Caco-2 cells, which express low levels of *CALIC* (Figs EV1D and EV2B and C). Thus, AXL expression may be regulated in a cell-type-specific manner. It is possible that the expression levels of other factors, including hnRNP-L, may be important for AXL expression.

To investigate the mechanism of *CALIC*/hnRNP-L-mediated AXL upregulation, we performed luciferase assays with reporter

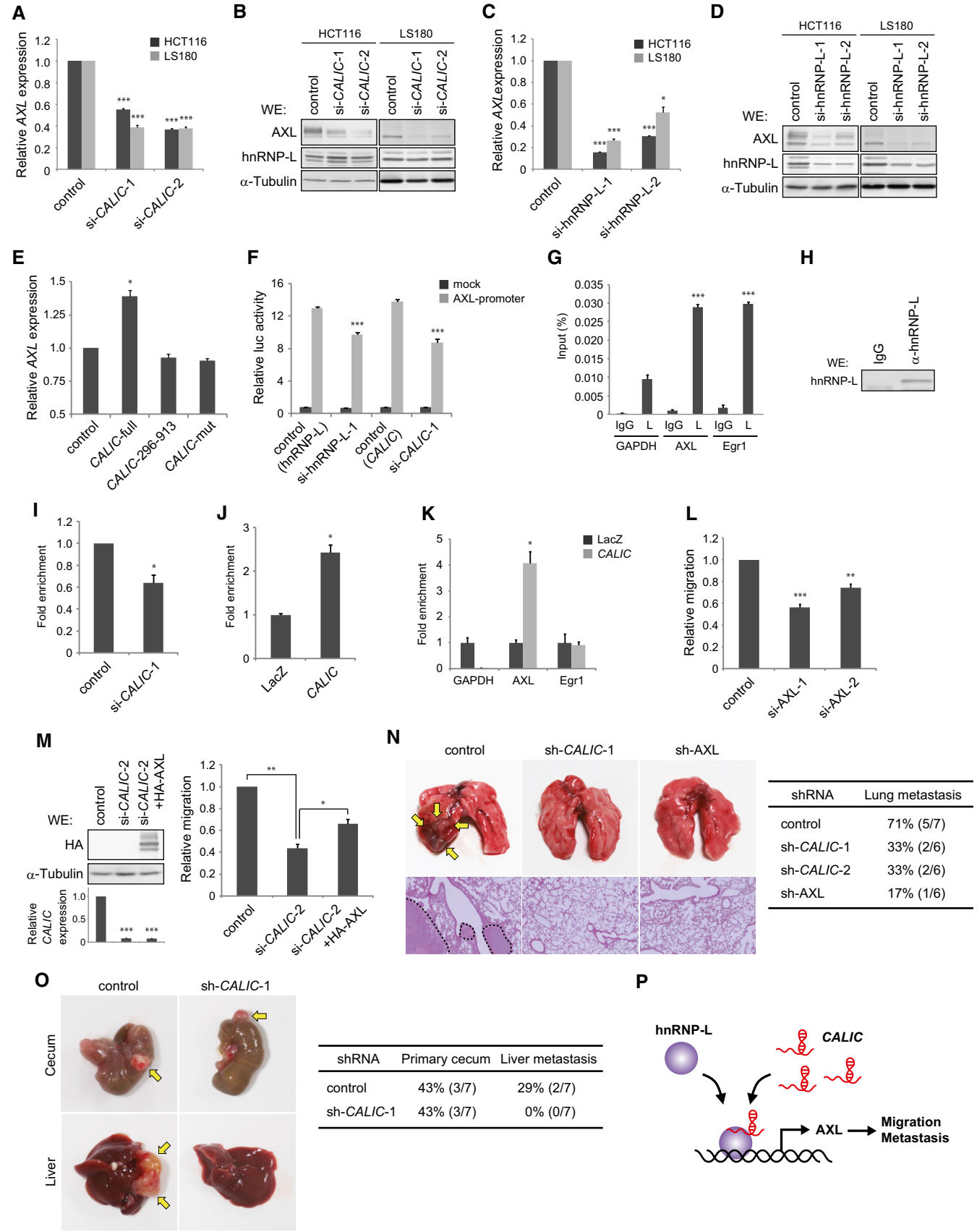

shRNA	Lung metastasis
control	71% (5/7)
sh-*CALIC*-1	33% (2/6)
sh-*CALIC*-2	33% (2/6)
sh-AXL	17% (1/6)

shRNA	Primary cecum	Liver metastasis
control	43% (3/7)	29% (2/7)
sh-*CALIC*-1	43% (3/7)	0% (0/7)

Figure 4.

Figure 4. Upregulation of AXL is essential for *CALIC*-mediated migration and metastasis.

A–D qRT–PCR (A, C) and immunoblotting (B, D) analyses of AXL in HCT116 and LS180 cells transfected with an siRNAs targeting *CALIC* or hnRNP-L (n = 3–4).

E qRT–PCR analyses of AXL in HCT116 cells infected with a lentivirus expressing wild-type *CALIC* (*CALIC*-full), *CALIC*-296-913, or *CALIC*-mut (see Fig 2B) (n = 3).

F HCT116 cells that had been treated with an siRNA targeting hnRNP-L or *CALIC* were transfected with an AXL reporter construct and subjected to luciferase assays (n = 4).

G, H ChIP assays were performed using anti-hnRNP-L antibody or control mouse IgG. The promoter regions of *GAPDH* and *Egr1* were used as negative and positive controls, respectively. Immunoblotting analysis of proteins precipitated by ChIP assays using anti-hnRNP-L antibody (H) (n = 4).

I ChIP analysis of hnRNP-L association with the AXL promoter region in *CALIC* knockdown HCT116 cells (n = 4).

J ChIP analysis of hnRNP-L association with the AXL promoter region in HCT116 cells expressing lentiviral *CALIC*-full (n = 3).

K ChIRP analysis of *CALIC* binding to the AXL promoter. Binding of *CALIC* to the promoter regions of the indicated genes was compared with that of LacZ (n = 3).

L Migratory activity of AXL knockdown HCT116 cells (n = 4).

M Lentiviral expression of AXL restores the migration activity of HCT116 cells transfected with an siRNA targeting *CALIC*. Immunoblotting and qRT–PCR analyses of HA-tagged AXL and *CALIC* expression, respectively (left). α-Tubulin was used as a loading control (n = 3).

N Representative images of gross specimens (top) and H&E-stained sections (bottom) of lung metastatic lesions in mice injected with *CALIC* or AXL knockdown HCT116 cells. Tumors were marked with yellow arrows. The dashed lines depict the boundary between normal and tumor tissues. (Right) Percentage of mice with lung metastases.

O Representative images of gross specimens of primary cecal tumors (top) and liver metastatic lesions (bottom) in mice orthotopically (cecal) injected with *CALIC* knockdown HCT116 cells. Tumors are marked with yellow arrows. (Right) Percentage of mice with primary tumors and liver metastases.

P A schematic model showing the mechanism of AXL regulation by *CALIC* and hnRNP-L. *CALIC* interacts with hnRNP-L to induce AXL expression and thereby facilitates metastasis.

Data information: Results are expressed as the mean ± SEM. *$P < 0.05$, **$P < 0.01$, ***$P < 0.001$ (Student's t-test).
Source data are available online for this figure.

constructs containing the AXL promoter region and found that knockdown of either hnRNP-L or *CALIC* suppressed AXL promoter activity in HCT116 cells (Fig 4F). Chromatin immunoprecipitation (ChIP) experiments using an anti-hnRNP-L antibody revealed that hnRNP-L is associated with the AXL promoter region, as well as a known target, the Egr1 promoter region (Fig 4G and H). Knockdown of *CALIC* reduced the occupancy of hnRNP-L at the AXL promoter region (Fig 4I). In contrast, overexpression of *CALIC* increased the occupancy of hnRNP-L on the AXL promoter (Fig 4J). ChIRP assays also showed that *CALIC* can bind to the AXL promoter region where hnRNP-L binds, but not to the promoter region in Egr1 (Fig 4K). These results suggest that *CALIC* promotes the recruitment of hnRNP-L to the AXL promoter region.

CALIC/hnRNP-L-mediated upregulation of AXL is essential for the metastatic behavior of colon cancer cells

Since AXL plays critical roles in migration, invasion, and metastasis [17,18], we investigated whether *CALIC*/hnRNP-L-mediated upregulation of AXL is responsible for the migratory activity of HCT116 cells. Consistent with previous reports [33], knockdown of AXL caused a reduction in HCT116 migratory activity (Figs 4L and EV2D). Furthermore, we observed that overexpression of AXL partially rescued the *CALIC* knockdown-induced reduction in HCT116 migration (Fig 4M). In addition, knockdown of neither *CALIC* nor *AXL* affected cell proliferation during the time course of migration assays (Fig EV2E). These results suggest that *CALIC* causes aberrant migration of colon cancer cells partially through AXL upregulation.

Finally, to determine the importance of *CALIC* in tumor metastasis, we examined metastasis of HCT116 cells infected with a lentivirus expressing an shRNA targeting *CALIC*. When control cells were intravenously injected into seven nude mice, metastatic lesions were detected in the lungs of five mice (71%) (Figs 4N and EV2F). However, mice injected with *CALIC* knockdown cells had less metastases [two out of six mice (33%)] than control mice. We obtained similar results using AXL knockdown cells [one out of six mice (17%)]. Furthermore, *CALIC* knockdown also suppressed liver metastasis when HCT116 cells were injected into the cecal wall of mice (Fig 4O). Taken together, our findings suggest that *CALIC* interacts with hnRNP-L to directly induce AXL expression and thereby promotes the metastatic ability of colon cancer cells (Fig 4P).

In this study, we identified *CALIC* as a lncRNA upregulated in metastatic subpopulations of a colon cancer cell line and demonstrated that *CALIC* is required for the metastasis of colon tumor cells. Furthermore, we showed that *CALIC* binds to and recruits hnRNP-L to the AXL promoter region and thereby upregulates its expression. There is no homology between *CALIC* and the AXL promoter region, excluding their direct base pairing. The molecular mechanisms by which the *CALIC*/hnRNP-L complex recognizes the AXL promoter region and upregulates AXL remain to be investigated.

Consistent with previous reports [17,18], our results suggested that the *CALIC*/hnRNP-L complex-mediated upregulation of AXL is critical for the metastatic ability of colon cancer cells. It has also been shown that AXL plays important roles in regulating cell growth, survival, and drug resistance [17,18]. It is therefore possible that *CALIC* also exerts critical roles in cell growth, survival, and drug resistance.

hnRNPs are often expressed abundantly and ubiquitously in cells and tissues [34]. By contrast, many lncRNAs are expressed in a tissue- and cancer-type restricted manner. Thus, lncRNAs associated with hnRNP family members may determine the functional specificity of hnRNPs. Consistent with this notion, we found that *CALIC* confers specificity to hnRNP-L. Similarly, *MYU* interacts with hnRNP-K to stabilize CDK6 expression and thereby promotes the G1-S transition of the cell cycle [35]. *FIRRE* induced by NF-κB signaling binds to hnRNP-U to regulate the stability of *VCAM1* and *IL12p40* mRNAs in macrophages and intestinal epithelial cells [36]. It is therefore possible that recruitment of hnRNPs to the target sites might be a common mechanism for a subset of lncRNAs to confer promoter specificity onto hnRNPs.

In conclusion, we have shown that the *CALIC*/hnRNP-L complex-mediated upregulation of AXL is critical for the metastasis of colon cancer cells. Thus, *CALIC* may be a promising molecular target for the therapy of colon cancers.

Materials and Methods

Cell culture and antibodies

HCT116 (ATCC) cells were cultured in McCoy's 5A medium supplemented with 10% FCS. LS180 (ATCC), WiDr (ATCC), and 293FT (Life Technologies, Frederick, MD, USA) cells were cultured in Dulbecco's modified Eagle's medium (DMEM) supplemented with 10% FCS. Colo320 (ATCC) cells were cultured in RPMI 1640 medium supplemented with 10% FCS. Caco-2 cells were cultured in Eagle's minimum essential medium (MEM) supplemented with 10% FCS and 0.1 mM non-essential amino acids. Mouse monoclonal (mAb) and rabbit polyclonal (pAb) antibodies against hnRNP-L were obtained from Abcam (Cambridge, MA, USA). Rabbit mAb to AXL and rat mAb to HA tag were from Cell Signaling Technology (Beverly, MA, USA) and Roche Applied Science (Mannheim, Germany), respectively. Mouse mAb to α-tubulin and lamin A/C were from Calbiochem (San Diego, CA, USA) and Santa Cruz Biotechnology (Santa Cruz, CA, USA), respectively.

Mice

Mouse experiments were approved by the Ethics Committee of the Institute of Molecular and Cellular Biosciences, The University of Tokyo, and were performed according to "the Guidelines for Proper Conduct of Animal Experiments" provided by the Science Council of Japan. Female BALB/cA nude mice were obtained from CLEA Japan (Tokyo, Japan). Animals were randomly assigned to cages.

Transfection of siRNAs

Silencer siRNAs (hnRNP-L-1, s6740; hnRNP-L-2, s6741; AXL-1, s1845; AXL-2, s1846, Ambion) and custom-made siRNAs (*CALIC*-1 and *CALIC*-2, Cosmo Bio) were transfected using Lipofectamine RNAiMAX (Life Technologies) 30 h after seeding. All siRNAs used in Fig 1C were chemically synthesized by Gene Design Inc (Osaka, Japan). Silencer negative control 1 siRNA (Ambion, Austin, TX, USA) and luciferase-control siRNA [Cosmo Bio (Tokyo, Japan) and Gene Design Inc] were used as negative controls. Sequences of custom-made siRNAs are listed in Table EV2.

Immunoblotting analyses and Cell migration assays

Immunoblotting analyses and cell migration assays were performed as described previously [37]. For cell migration using Transwell chambers (diameter 6.5 mm; pore size 8 μm; Costar Corporation, Cambridge, MA, USA), the underside of the membrane was coated with collagen type I (30 μg/ml) (Koken, Tokyo, Japan) for 12 h at 37°C. For the experiments using WiDr cells, the top chamber was coated by spotting fibronectin (100 ng) in 10 μl of phosphate-buffered saline onto the underside of the filter membrane, allowed to air-dry, and both sides of the membrane were then coated with collagen type I overnight. Cells (cells per well: HCT116, 5.0×10^3; WiDr, 5.0×10^4, Caco-2, 5.0×10^3; Colo320, 1.5×10^4) were added to the upper compartment of Transwell chambers and allowed to migrate to the underside of the top chamber for 7 h.

RNA isolation, qRT–PCR, RNA pull-down assays, RNA immunoprecipitation (RIP) assays, and Chromatin immunoprecipitation (ChIP) assays

RNA isolation, qRT–PCR, RNA pull-down assays, RIP assays, and ChIP assays were performed as described previously [35]. Primer sequences for quantitative PCR are listed in Table EV2. Colon cancer TissueScan qPCR arrays containing cDNAs from normal and cancer tissues were purchased from OriGene Technologies.

RNA-Seq and analysis

Total RNA was prepared using TRIsure reagent. cDNA libraries were prepared using the Illumina TruSeq Stranded Total RNA with Ribo-Zero Gold LT Sample Prep Kit. All libraries were sequenced using an Illumina Hiseq 2500 to create single-end 65 bp reads, which were aligned to the human reference genome build hg38 with STAR [38]. RSEM [39] was used to calculate transcripts per kilobase million (TPM, Ensembl gene annotation GRCh38). For differential expression analysis, we applied the count data to edgeR [40]. The count data were fitted with a general linear model. Gene ontology (GO) enrichment analysis was performed using DAVID [41]. Gene set enrichment analysis (GSEA) was performed using GSEA v3.0 (http://www.broad.mit.edu/gsea/).

Cell fractionation

Cells were washed with cold PBS and suspended in buffer A (10 mM HEPES pH 7.4, 10 mM KCl, 1.5 mM $MgCl_2$, 1 mM DTT). The cells were passed through a 25G needle 10 times, and homogenates were centrifuged at 1,000 *g* for 10 min to prepare the cytoplasmic and nuclear fractions.

Reporter assays

The promoter region of AXL (from −358 to +37) was amplified by PCR using corresponding specific primers and cloned into pGL4.20 (Promega, Madison, WI, USA). Luciferase assays were performed using the Dual Luciferase Assay System (Promega). pRL-TK was used as an internal control for the experiments.

Chromatin isolation by RNA purification

Chromatin isolation by RNA purification assays were performed as described [42]. Briefly, cells were cross-linked with 1% glutaraldehyde for 10 min at room temperature and then quenched with 0.125 M glycine for 5 min. Cross-linked RNA–chromatin was isolated and prepared for subsequent hybridization. Biotin-labeled antisense oligos were added to the RNA–chromatin extract, and they were incubated at 37°C for 4 h with rotation. RNA–chromatin complex was captured by incubation with streptavidin beads (Thermo Fischer Scientific, Waltham, MA, USA), and bead-associated RNA, DNA, and proteins were purified and analyzed by

qRT–PCR or immunoblotting. Biotinylated tiling oligos complementary to *lacZ* were used as a negative control for pull-down. ChIRP oligos are listed in Table EV2.

Lentiviral expression system

Lentiviral vector (CS-Rfa-CG) harboring an shRNA driven by the H1 promoter was generated using Gateway Technology (Life Technologies, Gaithersburg, MD, USA) and transfected with the packaging vectors pCAG-HIV-gp and pCMV-VSV-G-RSV-Rev into 293FT cells. The expression of lentiviral AXL and wild-type and mutant *CALIC* (nucleotide 296–913) were driven by the elongation factor-1 (EF1) promoter. All plasmids were kindly provided by H. Miyoshi (RIKEN BioResource Center, Japan). Virus supernatants were purified by ultracentrifugation and dissolved in PBS. HCT116 cells were infected with a lentivirus for 1 h at 37°C. Infected cells were cultured for more than 3 days before use in experiments. A lentivirus expressing LacZ or shRNA targeting luciferase was used as a negative control, respectively. Oligonucleotide sequences of shRNAs are listed in Table EV2.

In vivo metastasis assays and histology

HCT116 cells infected with a lentivirus were suspended in PBS and injected (2×10^6 cells/mouse) into the tail vein of 7-week-old nude mice. Mice were euthanized 7 weeks after injection, and lungs were excised to examine for possible metastases. For the orthotopic model, cells (2×10^6 cells/mouse) were injected into the cecal wall of nude mice. Liver and cecum were harvested 3 months after implantation. Paraffin-embedded sections from tissues were stained with hematoxylin and eosin (H/E).

Statistical analyses

Statistical analysis was performed using the Mann–Whitney *U*-test or Student's *t*-test. A P-value < 0.05 was considered to be statistically significant. Overall survival and disease-free survival were analyzed by GEPIA tool based on TCGA database.

Data availability

All raw sequence data (FASTQ format) are deposited in the DDBJ database under accession numbers DRA008353.

Expanded View for this article is available online.

Acknowledgements
This research was supported in part by a Grant-in-Aid for Scientific Research (B) (Grant No. 16H04692) from the Japan Society for the Promotion of Science (JSPS), Japan, the Core Research for Evolutional Science and Technology (CREST. Grant No. JPMJCR1863) from the Japan Science and Technology Agency (JST), and a grant from the Yasuda Medical Foundation (to YK). This work was also supported by a Grants-in-Aid for Scientific Research on Innovative Areas (Grant No. 17H06325) from MEXT, Japan, and the Project for Development of Innovative Research on Cancer Therapeutics (P-CREATE. Grant No. 17cm0106103h0002) from the Japan Agency for Medical Research and Development (AMED) (to TA).

Author contributions
YK, MM, TO, KM, and SS performed the experiments. LN performed the mass spectrometry analysis. RN, NY, and KS performed bioinformatics analyses. YK and TA analyzed the data and wrote the paper.

Conflict of interest
The authors declare that they have no conflict of interest.

References

1. Djebali S, Davis CA, Merkel A, Dobin A, Lassmann T, Mortazavi A, Tanzer A, Lagarde J, Lin W, Schlesinger F *et al* (2012) Landscape of transcription in human cells. *Nature* 489: 101 – 108
2. Esteller M (2011) Non-coding RNAs in human disease. *Nat Rev Genet* 12: 861 – 874
3. Derrien T, Johnson R, Bussotti G, Tanzer A, Djebali S, Tilgner H, Guernec G, Martin D, Merkel A, Knowles DG *et al* (2012) The GENCODE v7 catalog of human long noncoding RNAs: analysis of their gene structure, evolution, and expression. *Genome Res* 22: 1775 – 1789
4. Kapranov P, Cheng J, Dike S, Nix DA, Duttagupta R, Willingham AT, Stadler PF, Hertel J, Hackermüller J, Hofacker IL *et al* (2007) RNA maps reveal new RNA classes and a possible function for pervasive transcription. *Science* 316: 1484 – 1488
5. Kopp F, Mendell JT (2018) Functional Classification and Experimental Dissection of Long Noncoding RNAs. *Cell* 172: 393 – 407
6. Anastasiadou E, Jacob LS, Slack FJ (2018) Non-coding RNA networks in cancer. *Nat Rev Cancer* 18: 5 – 18
7. Wong CM, Tsang FH, Ng IO (2018) Non-coding RNAs in hepatocellular carcinoma: molecular functions and pathological implications. *Nat Rev Gastroenterol Hepatol* 15: 137 – 151
8. Batista PJ, Chang HY (2013) Long noncoding RNAs: cellular address codes in development and disease. *Cell* 152: 1298 – 1307
9. Huarte M (2015) The emerging role of lncRNAs in cancer. *Nat Med* 21: 1253 – 1261
10. Goff LA, Rinn JL (2015) Linking RNA biology to lncRNAs. *Genome Res* 25: 1456 – 1465
11. Ransohoff JD, Wei Y, Khavari PA (2018) The functions and unique features of long intergenic non-coding RNA. *Nat Rev Mol Cell Biol* 19: 143 – 157
12. Kim TK, Shiekhattar R (2016) Diverse regulatory interactions of long noncoding RNAs. *Curr Opin Genet Dev* 36: 73 – 82
13. Chaffer CL, Weinberg RA (2011) A perspective on cancer cell metastasis. *Science* 331: 1559 – 1564
14. Massagué J, Obenauf AC (2016) Metastatic colonization by circulating tumour cells. *Nature* 529: 298 – 306
15. Goruppi S, Ruaro E, Varnum B, Schneider C (1999) Gas6-mediated survival in NIH3T3 cells activates stress signalling cascade and is independent of Ras. *Oncogene* 18: 4224 – 4236
16. Grommes C, Lee CY, Wilkinson BL, Jiang Q, Koenigsknecht-Talboo JL, Varnum B, Landreth GE (2008) Regulation of microglial phagocytosis and inflammatory gene expression by Gas6 acting on the Axl/Mer family of tyrosine kinases. *J Neuroimmune Pharmacol* 3: 130 – 140
17. Graham DK, DeRyckere D, Davies KD, Earp HS (2014) The TAM family: phosphatidylserine sensing receptor tyrosine kinases gone awry in cancer. *Nat Rev Cancer* 14: 769 – 785
18. Wu X, Liu X, Koul S, Lee CY, Zhang Z, Halmos B (2014) AXL kinase as a novel target for cancer therapy. *Oncotarget* 5: 9546 – 9563

19. Nguyen DX, Chiang AC, Zhang XH, Kim JY, Kris MG, Ladanyi M, Gerald WL, Massagué J (2009) WNT/TCF signaling through LEF1 and HOXB9 mediates lung adenocarcinoma metastasis. *Cell* 138: 51 – 62
20. Malladi S, Macalinao DG, Jin X, He L, Basnet H, Zou Y, de Stanchina E, Massagué J (2016) Metastatic Latency and Immune Evasion through Autocrine Inhibition of WNT. *Cell* 165: 45 – 60
21. Kong L, Zhang Y, Ye ZQ, Liu XQ, Zhao SQ, Wei L, Gao G (2007) CPC: assess the protein-coding potential of transcripts using sequence features and support vector machine. *Nucleic Acids Res* 35: W345 – W349
22. Wang L, Park HJ, Dasari S, Wang S, Kocher JP, Li W (2013) Cpat: coding-potential assessment tool using an alignment-free logistic regression model. *Nucleic Acids Res* 41: e74
23. Tripathi V, Ellis JD, Shen Z, Song DY, Pan Q, Watt AT, Freier SM, Bennett CF, Sharma A, Bubulya PA *et al* (2010) The nuclear-retained noncoding RNA MALAT1 regulates alternative splicing by modulating SR splicing factor phosphorylation. *Mol Cell* 39: 925 – 938
24. Zheng G, Ma Y, Zou Y, Yin A, Li W, Dong D (2018) HCMDB: the human cancer metastasis database. *Nucleic Acids Res* 46: D950 – D955
25. Motta-Mena LB, Heyd F, Lynch KW (2010) Context-dependent regulatory mechanism of the splicing factor hnRNP L. *Mol Cell* 37: 223 – 234
26. Yao P, Wu J, Lindner D, Fox PL (2017) Interplay between miR-574-3p and hnRNP L regulates VEGFA mRNA translation and tumorigenesis. *Nucleic Acids Res* 45: 7950 – 7964
27. Ruan X, Li P, Cangelosi A, Yang L, Cao H (2016) A Long Non-coding RNA, lncLGR, Regulates Hepatic Glucokinase Expression and Glycogen Storage during Fasting. *Cell Rep* 14: 1867 – 1875
28. Li Z, Chao TC, Chang KY, Lin N, Patil VS, Shimizu C, Head SR, Burns JC, Rana TM (2014) The long noncoding RNA THRIL regulates TNFα expression through its interaction with hnRNPL. *Proc Natl Acad Sci USA* 111: 1002 – 1007
29. Huang Y, Li W, Yao X, Lin QJ, Yin JW, Liang Y, Heiner M, Tia B, Hui J, Wang G (2012) Mediator complex regulates alternative mRNA processing via the MED23 subunit. *Mol Cell* 45: 459 – 469
30. Atianand MK, Hu W, Satpathy AT, Shen Y, Ricci EP, Alvarez-Dominguez JR, Bhatta A, Schattgen SA, McGowan JD, Blin J *et al* (2016) A Long Noncoding RNA lincRNA-EPS Acts as a Transcriptional Brake to Restrain Inflammation. *Cell* 165: 1672 – 1685
31. Guang S, Felthauser AM, Mertz JE (2005) Binding of hnRNP L to the pre-mRNA processing enhancer of the herpes simplex virus thymidine kinase gene enhances both polyadenylation and nucleocytoplasmic export of intronless mRNAs. *Mol Cell Biol* 25: 6303 – 6313
32. Hui J, Stangl K, Lane WS, Bindereif A (2003) HnRNP L stimulates splicing of the eNOS gene by binding to variable-length CA repeats. *Nat Struct Biol* 10: 33 – 37
33. Dunne PD, McArt DG, Blayney JK, Kalimutho M, Greer S, Wang T, Srivastava S, Ong CW, Arthur K, Loughrey M *et al* (2014) AXL is a key regulator of inherent and chemotherapy-induced invasion and predicts a poor clinical outcome in early-stage colon cancer. *Clin Cancer Res* 20: 164 – 175
34. Geuens T, Bouhy D, Timmerman V (2016) The hnRNP family: insights into their role in health and disease. *Hum Genet* 135: 851 – 867
35. Kawasaki Y, Komiya M, Matsumura K, Negishi L, Suda S, Okuno M, Yokota N, Osada T, Nagashima T, Hiyoshi M *et al* (2016) MYU, a Target lncRNA for Wnt/c-Myc Signaling, Mediates Induction of CDK6 to Promote Cell Cycle Progression. *Cell Rep* 16: 2554 – 2564
36. Lu Y, Liu X, Xie M, Liu M, Ye M, Li M, Chen XM, Li X, Zhou R (2017) The NF-κB-Responsive Long Noncoding RNA FIRRE Regulates Posttranscriptional Regulation of Inflammatory Gene Expression through Interacting with hnRNPU. *J Immunol* 199: 3571 – 3582
37. Kawasaki Y, Sato R, Akiyama T (2003) Mutated APC and Asef are involved in the migration of colorectal tumour cells. *Nat Cell Biol* 5: 211 – 215
38. Dobin A, Davis CA, Schlesinger F, Drenkow J, Zaleski C, Jha S, Batut P, Chaisson M, Gingeras TR (2013) STAR: ultrafast universal RNA-seq aligner. *Bioinformatics* 29: 15 – 21
39. Li B, Dewey CN (2011) RSEM: accurate transcript quantification from RNA-Seq data with or without a reference genome. *BMC Bioinformatics* 12: 323
40. Zhou X, Lindsay H, Robinson MD (2014) Robustly detecting differential expression in RNA sequencing data using observation weights. *Nucleic Acids Res* 42: e91
41. da Huang W, Sherman BT, Lempicki RA (2009) Bioinformatics enrichment tools: paths toward the comprehensive functional analysis of large gene lists. *Nucleic Acids Res* 37: 1 – 13
42. Chu C, Qu K, Zhong FL, Artandi SE, Chang HY (2011) Genomic maps of long noncoding RNA occupancy reveal principles of RNA-chromatin interactions. *Mol Cell* 44: 667 – 678

